2026 IEEE/SICE International Symposium on System Integration (SII)
January 11-14, 2026. Cancún, México

Fully Automated CAD/BIM Modeling of Pipe Structures from Plant Environment 3D Point Cloud

Takashi Imabuchi, *Member, IEEE* and Kuniaki Kawabata, *Senior Member, IEEE*

Abstract— **This paper describes a fully automated method for generating 3D pipe models with wall thickness from 3D point cloud data. In decommissioning of Fukushima Daiichi Nuclear Power Station, rapid 3D modeling of plant structures is essential for dose assessment and remote operation planning. In our method, pipe regions are first discriminated, then scanned along three orthogonal axes to extract pipe instances, followed by geometric fitting with wall thickness for use in shielding calculations. Finally, generated models are exported in Computer-Aided Design (CAD) and Building Information Modeling (BIM) formats for using facility management. Our method was validated on a 3D point cloud measured in a mock-up plant environment. We confirmed a high conversion rate and reduced processing time by restricting computation to pipe regions. The output models were imported into existing software without errors.**

I. Introduction

In the decommissioning of the Fukushima Daiichi Nuclear Power Station (FDNPS) owned by Tokyo Electric Power Company Holdings, Inc., the first trial retrieval of fuel debris from the Primary Containment Vessel of Unit 2 was completed in 2024 [1]. In the coming years, large-scale fuel debris retrieval operations will be conducted for Units 1-3. Such operations require activities including the consideration of construction methods, planning of remotely robot operations, and radiation dose calculations based on structural information. These tasks utilize 3D models created from 3D point cloud acquired in the work environment using 3D laser scanners. However, converting 3D point cloud into 3D models still relies heavily on manual operations with dedicated software, which is highly time- and labor-intensive. For safe and efficient decommissioning, it is essential to carry out operations appropriately while promptly incorporating up-to-date site conditions to models that change from moment to moment.

In particular, understanding the radiation condition in the work environment is crucial for reducing exposure to workers and remotely operated equipment, and radiation dose calculations using 3D models of structures are highly valuable [2]. Such calculations require not only information on the arrangement and geometry of structures but also data on the constituent materials and their thicknesses. However, the created 3D models (commonly in Computer-Aided Design (CAD) format) are often surface models, with no representation of the interior. When thickness information is absent, the 3D model treats structures as solid masses, which can lead to unintended shielding effects or inaccurate attenuation calculations [3]. At FDNPS, understanding contamination originating from inside piping is a critical issue, highlighting the need for an easy method to create 3D models with wall thickness. Representing the interior of shapes such as pipes and pumps is far more challenging—and significantly more costly—than modeling simple structures like flat walls. Material information, on the other hand, directly contributes to the accuracy of shielding calculations. Recently, attention has also been drawn to the use of Building Information Modeling (BIM) models, which can incorporate such material and thickness information.

Against this background, we have been working on the development of an automated method for generating 3D models from 3D point cloud. In previous works, we have developed a method that automatically discriminates structures from 3D point cloud into categories and segments them into shape regions, and we have confirmed high discrimination accuracy for major categories in plant environment datasets [4, 5]. Although discrimination performance was low for categories with insufficient training data, however, the “pipe” category achieved more than 90% accuracy. We believe the process of segmenting parts in 3D models can be streamlined by utilizing predicted shape regions shape regions by category. Compared with conventional algorithms that search for target models over the entire 3D point cloud [6], our approach is expected to improve both accuracy and processing speed. Commercial software packages provide semi-automatic tools for piping model generation; however, these typically require extensive manual editing, particularly when 3D point cloud contain occlusions, noise, or incomplete coverage [7].

In this paper, we demonstrate a fully automated method for 3D modeling of pipes from 3D point cloud acquired in plant environments. By using point cloud discrimination to extract target pipes and performing model fitting, our method is expected to prevent incorrect modeling of non-pipe structures and achieve faster processing. In comparison of traditional works, our method offers full automation, explicit wall thickness modeling, and direct CAD/BIM-compatible output. In the verification, we confirmed that our method operates effectively using 3D point cloud data from a mock-up plant environment that replicates representative structures at the FDNPS, and we also demonstrate that the generated models can be successfully imported into existing software.

II. Method

In this section, we describe an automated method for generating 3D models of pipes from 3D point cloud. Figure 1

All authors are with Fukushima Research and Engineering Institute, Japan Atomic Energy Agency (JAEA), Fukushima, Japan (phone: (+81)240-26-1188; e-mail: imabuchi.takashi@jaea.go.jp).

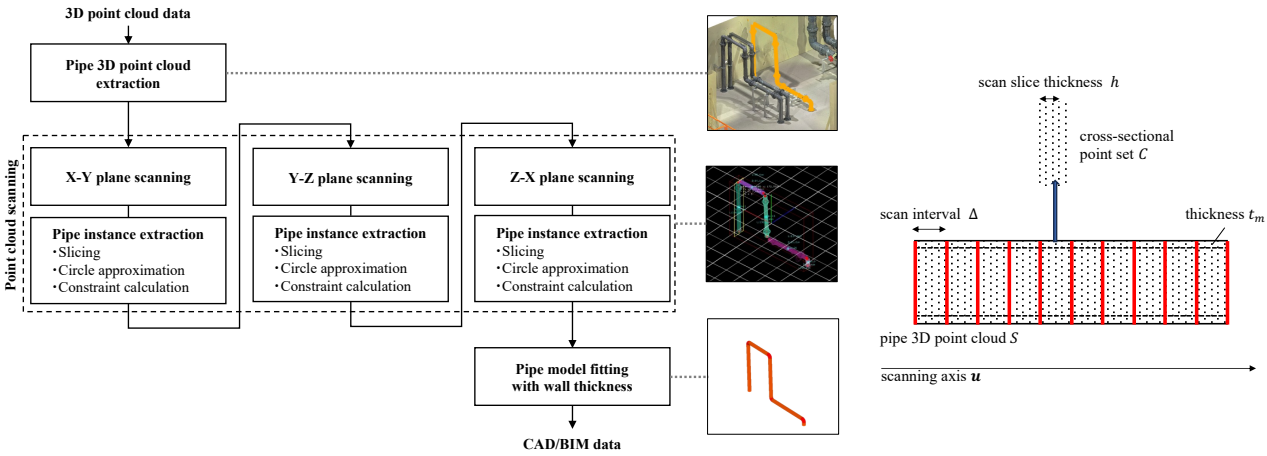

(a) Overview of processing (b) relationship between parameters

Figure 1. Fully automated pipe 3D modeling method.

(a) shows a processing flow. The method begins by extracting the target pipes to be modeled from the 3D point cloud by our previous method [4]. Next, point cloud scanning is performed along three orthogonal axes on the pipe segments to extract individual pipe instances. When a floor and wall-based coordinate system is employed, pipes are typically aligned with its principal axes, and slicing is expected to enable effective extraction of their continuity. Finally, model fitting with wall thickness representation is applied to each pipe instance. The following subsections detail the point cloud scanning process and the model fitting procedure.

A. Point Cloud Scanning

In the process of point cloud scanning, the extracted pipe point cloud $S = \{\boldsymbol{p_i} \in \mathbb{R}^3\}_{i=1}^{N}$ is scanned along the three predefined orthogonal axes $\{\boldsymbol{e_x}, \boldsymbol{e_y}, \boldsymbol{e_z}\}$ to identify individual pipe instances and estimate their dimensions. Figure 1 (b) shows the relationship between parameters related to scanning. Given a scan interval Δ and slice thickness h, the coordinate of each point along a scanning axis $\boldsymbol{u}$ is computed as

$$t_i = \boldsymbol{u}^{\top}\boldsymbol{p_i}. \tag{1}$$

The scan positions are discretized as

$$t_k = t_{min} + k\Delta, \tag{2}$$

and a slice slab is defined by

$$\Pi_k = \{\boldsymbol{x} \in \mathbb{R}^3 \mid |\boldsymbol{u}^{\top}\boldsymbol{x} - t_k| \leq h/2\}. \tag{3}$$

The set of points within Π_k is taken as the cross-sectional point set:

$$C_k = \{\boldsymbol{p_i} \in S \mid |t_i - t_k| \leq h/2\}. \tag{4}$$

Each cross-section C_k is projected onto an orthonormal basis $(\boldsymbol{v_1}, \boldsymbol{v_2})$ perpendicular to $\boldsymbol{u}$, yielding

$$q_i^{(k)} = \left[x_i^{(k)}, y_i^{(k)}\right]^T. \tag{5}$$

The Taubin method is then applied to fit a circle

$$\mathcal{C}_k = (c_k, r_k) \tag{6}$$

with radius constraints $r_{min} \leq r_k \leq r_{max}$ uppers outliers [8]. The 3D circle center is reconstructed as

$$\hat{c}_k = \bar{p}_k + \boldsymbol{v_1}c_{x,k} + \boldsymbol{v_2}c_{y,k}, \tag{7}$$

where $\bar{p}_k$ is the centroid of C_k.

Continuity along the scan direction is evaluated using the center displacement

$$\delta_k = \|\hat{c}_k - \hat{c}_{k-1}\|_2 \tag{8}$$

and the radius variation

$$\Delta r_k = |r_k - r_{k-1}|, \tag{9}$$

with thresholds τ_c and τ_r, respectively. If either condition is violated, the current segment is terminated and its length endpoint is determined. For pipes oriented obliquely, the scanning axis is updated from the start and end centers $s = \hat{c}_k^{start}$, $e = \hat{c}_k^{end}$ via

$$\hat{\boldsymbol{u}} = \frac{e-s}{\|e-s\|_2} \tag{10}$$

and the slicing/fitting is re-run along $\hat{\boldsymbol{u}}$. Finally, instance segmentation applies a distance threshold τ_{split} to the sequence of centers $\{\hat{c}_k\}$, the per-instance radius is

$$\bar{r} = median\{r_k\}, \tag{11}$$

and the length is the endpoint distance.

B. Pipe Model Fitting with Wall Thickness

In the process of model fitting, each pipe instance $\mathcal{I}_m$ obtained from previous section is fitted with a cylindrical model, and a geometric representation is generated for use in CAD and BIM environments. From the center sequence $\{\hat{c}_k\}_{k\in\mathcal{I}_m}$, Total Least Squares yields the unit axis direction $\boldsymbol{a_m}$ and an axis point $\boldsymbol{o_m}$, defining the axis

$$l_m(\lambda) = \boldsymbol{o_m} + \lambda\boldsymbol{a_m},\ \lambda \in \mathbb{R}. \tag{12}$$

The radius is aggregated as

$$r_m = median\{r_k \mid k \in \mathcal{I}_m\}, \tag{13}$$

and the length as

(a) Photograph (b) Measured 3D point cloud

Figure 2. Mock-up plant environment and measured 3D point cloud

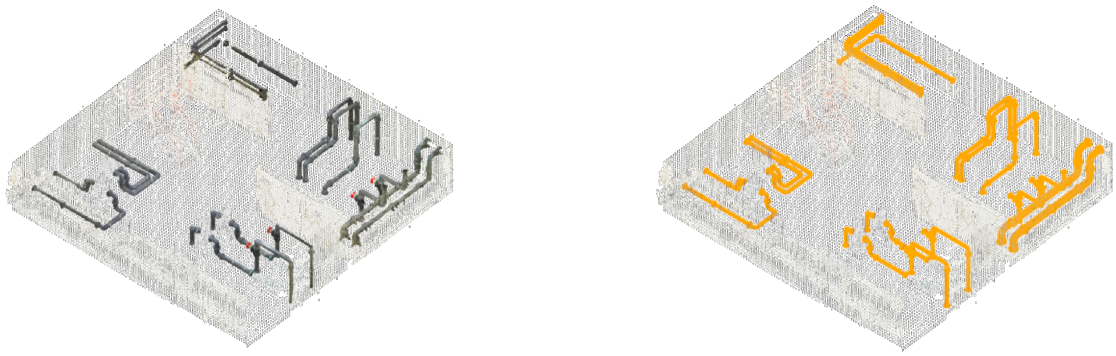

(a) Pipe point cloud (b) Ground-truth 3D model

Figure 3. Overview of pipe point cloud

$$L_m = \left\| \hat{c}_k^{start} - \hat{c}_k^{end} \right\|_2. \quad (14)$$

Given a thickness parameter t_m, we set outer/inner radii $r_m^{\text{out}} = r_m$, $r_m^{\text{in}} = r_m - t_m$ and define the parametric cylinder

$$\mathcal{M}_m = (\boldsymbol{o_m}, \boldsymbol{a_m}, r_m^{\text{out}}, r_m^{\text{in}}, L_m). \quad (15)$$

This thickness parameter is a predefined parameter uniformly applied to the generated pipe model. Therefore, it must be modified within the modeling software.

For CAD model generation, OpenCascade is employed to construct the outer and inner cylinders as Brep solids, and a Boolean subtraction is applied to form the hollow structure [9]. For BIM model generation, IfcOpenShell is used to create a profile from r_m^{out} and r_m^{in}, and assign it to an IFC pipe element [10].

III. Verification

In this section, we present the results of verifying the performance of the proposed method using 3D point cloud data acquired in a mock-up plant environment replicating structures at the plant facilities. The evaluation focuses on the conversion rate obtained when applying the proposed method to pre-extracted pipe point cloud, and discusses issues to be addressed in future work.

Figure 2 shows the mock-up plant environment and the measured 3D point cloud used in the verification. The mock-up plant environment covering an area of 10 m × 10 m was constructed in the test building of the Naraha Remote Technology Development Center of JAEA, [11]. The structures installed in the environment simulate representative on-site facilities, including piping, stairs, control panels, tanks, ducts, cables, slopes, and partition walls. In this verification, polyvinyl chloride pipes were selected as the target. The 3D point cloud shown in Figure 2(b) was measured from 26 locations using a FARO Focus S350 and registered using the dedicated FARO SCENE software [12]. The total number of points was 93,205,791.

To verify the performance of the proposed method, the portion of the point cloud corresponding to pipes was extracted as shown in Figure 3(a). The extracted point cloud contained 7,202,666 points, and the proposed method was applied to this dataset. The parameters were set as follows: scan interval Δ = 10 mm, slice thickness h = 10 mm, diameter constraint range r_{min} = 400, r_{max} = 50 mm, parameters about maximum allowable center displacement τ_c = τ_r = 30 mm, and wall thickness t_m = 10 mm.

A 3D model of the mock-up environment had been created at the design stage, and the pipe 3D model shown in Figure 3(b) was used as the ground-truth data for conversion rate calculation. The conversion rate was computed using surface mesh vertices uniformly sampled at 1 cm intervals on both the generated and ground-truth models (436,837 vertices), and calculating point-to-point distances. Completeness was used as the conversion rate of evaluation metric, defined as the percentage of generated vertices that were within a specified distance of any ground-truth vertex. Distances of 30, 50, 70, and 100 mm were used as thresholds. In addition, the processing time required to apply the method was measured. The specifications of the computer used for processing were: CPU – Intel Core i9-11900K (3.5 GHz), GPU – NVIDIA GeForce RTX 3090 (24 GB), and memory – 64 GB.

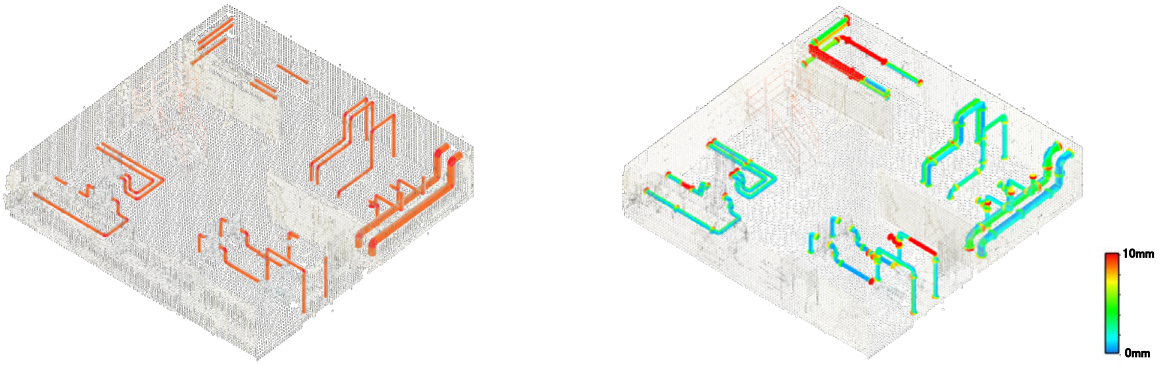

(a) Generated 3D Model (b) Point-to-point distance distribution

Figure 4. Overview of the generated pipe 3D model

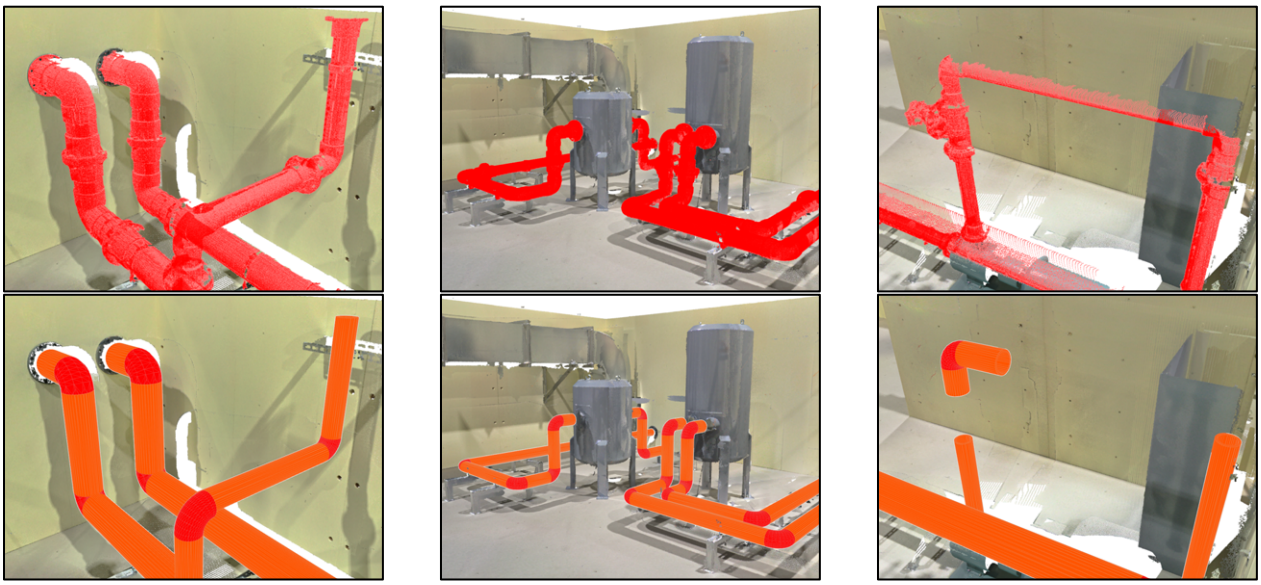

Figure 5. Example of a generated pipe 3D model (Top: 3D point cloud, Bottom: Generated 3Dmodel)

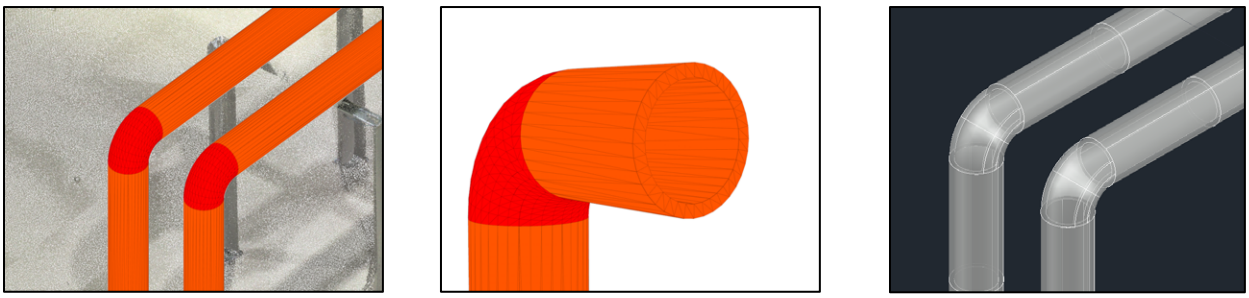

(a) Generated mesh model (b) Cross-section of mesh model (c) Generated CAD model

Figure 6. Thickness of pipe generation results

Figure 4(a) shows the 3D model generated using the proposed method, and Figure 4(b) presents the point-to-point distance distribution used for calculating the conversion rate. Table 1 summarizes the conversion rates. The verification results show that the conversion rate was 90.24% at a distance threshold of 10 cm, and 55.59% at a threshold of 3 cm. Figure 5 provides snapshots comparing the pipe point cloud and the generated model from the same viewpoint. Overall, the results confirm that pipes were generated in accordance with the point cloud. However, in areas where the pipe geometry was only partially captured or valve connection, circular fitting failed, and no pipe model was generated similar to previous studies.

TABLE I. THE RESULT OF CONVERSION RATE

Search distance	*Number of vertices*	*Completeness*
100mm	394,185	90.24%
70mm	369,345	84.55%
50mm	331,732	75.93%
30mm	242.837	55.59%

The reduction in conversion rate is mainly attributed to such missing segments and to deviations caused by noise that prevented accurate circular fitting. A more detailed shape reproducibility evaluations, such as diameter estimation error and center position error are needed in future work.

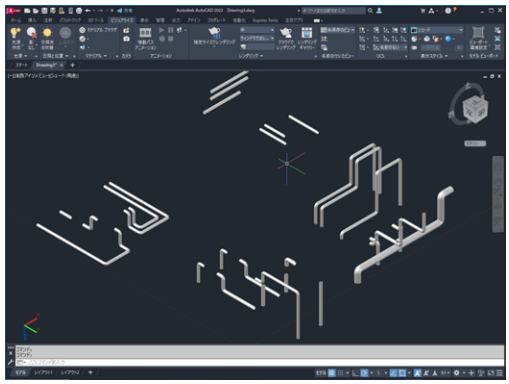

(a) CAD format data

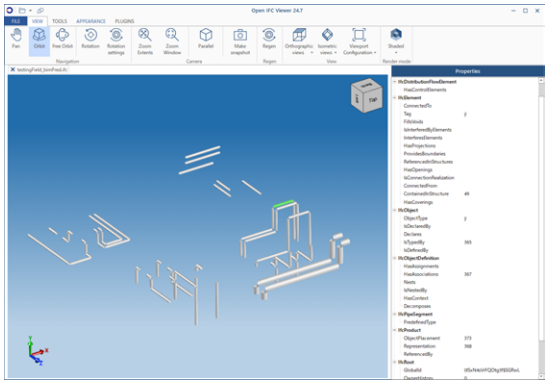

(b) BIM format data

Figure 7. Results of importing CAD/BIM format data generated by dedicated software

Additionally, since the missing segments were located between correctly generated pipe sections, we plan to investigate interpolation techniques to address these gaps.

The processing time was 290.5 seconds for point cloud scanning and 9.3 seconds for model fitting. Compared to conventional methods that scan the entire point cloud, applying our method enables high-speed processing by limiting the scan target to only the pipe's point cloud. The representation of pipe wall thickness is illustrated in Figure 6. Figure 6(a) shows generated meshed model, and Figure 6(b) presents a cross-sectional view of Figure 6(a). The generated CAD model is shown in Figure 6(c), and its interior can be observed through its semi-transparent display. As indicated, the results confirm that the generated model preserves internal wall thickness in both mesh and parametric representations. Finally, Figure 7 shows the results of importing the generated models into existing software. Figure 7(a) presents the CAD format model loaded in Autodesk AutoCAD [13], while Figure 7(b) shows the BIM format model loaded in OpenIFCViewer [14]. In both cases, the models were imported successfully without any errors.

IV. Conclusion

In this paper, we described a fully automated method for generating pipe 3D models with wall thickness to rapidly create 3D representations of decommissioning work environments. The method uses automatically discriminated target regions in 3D point cloud to fit pipes with wall thickness and exports the results in CAD and BIM formats. Experimental verification using a mock-up plant environment demonstrated that the proposed method can automatically generate pipe models with wall thickness from raw point cloud significantly reduce processing time by limiting computation to target regions, and produce outputs that can be seamlessly integrated into CAD/BIM-based workflows.

Future work will focus on clarifying positional accuracy, addressing incomplete point cloud, and extending the method to other structure categories such as pump, walls and othor equipment. Ultimately, we aim to deploy a prototype system for use in actual decommissioning operations.

Acknowledgement

This research is supported by the subsidy project for decommissioning, contaminated water, and treated water management expenses (Development of technologies for environmental improvement inside reactor buildings (Development of advanced technologies for digitizing the environment and source distribution to reduce exposure)) funded by the Ministry of Economy, Trade, and Industry, starting in fiscal year 2023.

References

[1] Fukushima Daiichi Nuclear Power Station Recommencement of the Unit 2 Fuel Debris Trial Retrieval (Completion of Fuel Debris Grasping Work): Tokyo Electric Power Company Holdings, Inc. https://photo.tepco.co.jp/en/date/2024-e/202410-e/241030-02e.html

[2] J. Lee, G.H. Kim, I. Kim, D. Hyun, K.S. Jeong, B.S. Choi, J. Moon, "Establishment of the framework to visualize the space dose rates on the dismantling simulation system based on a digital manufacturing platform," Annals of Nuclear Energy, vol.95, pp.161-167, 2016.

[3] T. Sato, K. Niita, N. Matsuda, S. Hashimoto, Y. Iwamoto, S. Noda, T. Ogawa, H. Iwase, H. Nakashima, T. Fukahori, K. Okumura, T. Kai, S. Chiba, T. Furuta, and L. Sihver, "Particle and Heavy Ion Transport Code System PHITS, Version 2.52," Journal of Nuclear Science and Technology, vol. 50, no. 9, pp. 913-923, 2013.

[4] T. Imabuchi, K. Kawabata, "Discrimination of structures in plant using deep learning models trained by 3D CAD semantics", Artif Life Robotics, Vol.30, pp.184-195, (2025). https://doi.org/10.1007/s10015-024-00989-w.

[5] T. Imabuchi, Kawabata, "Semantic and Volumetric 3D Plant Structures Modeling Using Projected Image of 3D Point Cloud", The 2024 IEEE/SICE International Symposium on System Integration (SII 2024), 2024.

[6] R. Schnabel, R. Wahl, and R. Klein, "Efficient RANSAC for Point-Cloud Shape Detection," Computer Graphics Forum, Vol.26, No.2, pp. 214-226, 2007. https://doi.org/10.1111/j.1467-8659.2007. 01016.x

[7] H. Son, C. Kim, Y. Turkan, "Scan-to-BIM - An Overview of the Current State of the Art and a Look Ahead," 2015 Proceedings of the 32nd International Symposium on · Automation and Robotics in Construction (ISARC2015), pp. 1-8 2015.

[8] G. Taubin, "Estimation of Planar Curves, Surfaces, and Non-planar Space Curves Defined by Implicit Equations with Applications to Edge and Rage Image Segmentation," IEEE Transactions on Pattern Analysis and Machine Intelligence, vol.13. no.11, pp.1115-1138, 1991.

[9] Open Cascade, part of Capgemini, https://www.opencascade.com

[10] IfcOpenShell - The open source IFC toolkit and geometry engine, https://ifcopenshell.org

[11] Japan Atomic Energy Agency Naraha Center for Remote Control Technology Development (NARREC), https://naraha.jaea.go.jp/en/index.html

[12] FARO 3D laser scanner, https://www.faro.com/ja-JP

[13] AutoCAD, https://www.autodesk.com/jp/products/autocad/overview

[14] Open IFC Viewer, https://openifcviewer.com